Neutrino mass hierarchy from the discrete dark matter model

Cesar Bonilla,[a] **Johannes Herms,**[b] **Omar Medina**[c,*] **and Eduardo Peinado**[d]

[a]*Departamento de Física, Universidad Católica del Norte,*
Avenida Angamos 0610, Casilla 1280, Antofagasta, Chile

[b]*Max-Planck-Institut für Kernphysik,*
Saupfercheckweg 1, 69117 Heidelberg, Germany

[c]*Institut de Física Corpuscular (CSIC-Universitat de València), AHEP Group,*
Parc Científic de Paterna, C/ Catedrático José Beltrán, 2 E-46980 Paterna (Valencia), Spain

[c]*Instituto de Física, Universidad Nacional Autónoma de México,*
A.P. 20-364, Ciudad de México 01000, México.

E-mail: Omar.Medina@ific.uv.es

We explore a possible explanation for the hierarchy in scale between the atmospheric and solar neutrino mass differences ($|\Delta m_{31}^2|$, and Δm_{21}^2) through the presence of two distinct neutrino mass mechanisms from tree- and one-loop-level contributions. We demonstrate that the ingredients needed to explain this hierarchy are present in the minimal discrete dark matter model [1]. This scenario is characterized by adding new RH neutrinos and scalar $SU(2)$ doublets to the Standard Model as triplet representations of an A_4 flavour symmetry. The A_4 symmetry breaking, which occurs at the electroweak scale, leads to a residual $\mathbb{Z}_2$ symmetry responsible for the dark matter stability and dictates the neutrino phenomenology. We show that CP breaking in the scalar potential is needed to fit the neutrino mixing angles.
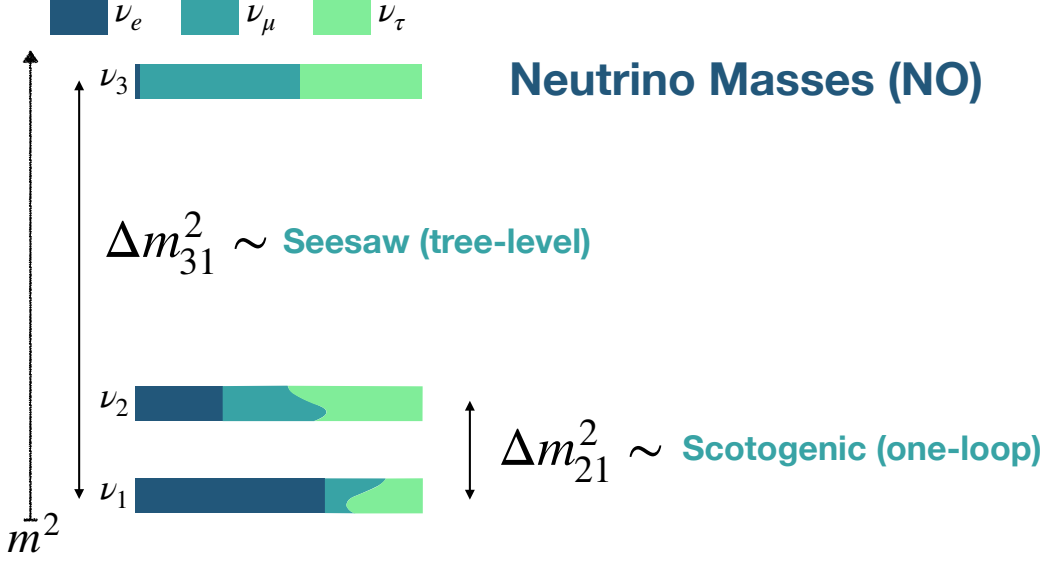
*Speaker

PoS(DISCRETE2022)076

Figure 1: In the discrete dark matter (DDM) model [1], the neutrino mass splittings $|\Delta m^2_{31}|$, and Δm^2_{21} are generated; by a seesaw, and a scotogenic mechanism respectively [5–7]. This figure illustrates how this model can naturally explain the hierarchy between these mass splittings and the neutrino mass ordering through the dominance of a tree-level mass mechanism over a loop-suppressed one.

1. Introduction

The origin of neutrino mass and the unknown nature of dark matter (DM) are strong evidence of physics beyond the standard model (BSM). Moreover, unscrambling the flavour puzzle present in the SM is essential for building a fundamental theory of particle interactions. It is so because most of the input parameters in the SM are directly related to flavour. With the unprecedented reduction of experimental uncertainties in the measurement of lepton mixing parameters [2], it has become increasingly compelling to explore models where these three issues are addressed together.

In this work, based on [1], we summarize the interesting features of the discrete dark matter model (DDM) [3, 4], which deals with the three issues mentioned above. This model is a SM extension with an A_4 flavour symmetry whose spontaneous breaking stabilizes a DM scalar particle candidate. We demonstrate that in this model, an interplay between two mass mechanisms (tree-level seesaw and one-loop scotogenic) emerges naturally from the A_4 symmetry and its breakdown. This feature of the model predicts Normal Ordering (NO) of neutrino masses and explains the hierarchy between the atmospheric $|\Delta m^2_{31}| \sim 2.55 \times 10^{-3}$ (NO), and the solar $\Delta m^2_{21} \sim 7.5 \times 10^{-5}$ mass splittings, which differ by two orders of magnitude [2]. This is illustrated in Figure 1.

This work is structured as follows. In Section 2 we outline the fields and symmetries of the model. In Section 3 we describe the neutrino mass mechanisms in the model. In Section 4 we summarize our results, and lastly Section 5 contains our conclusions.

2. The discrete dark matter model

This model extends the SM symmetry group by an A_4 flavor symmetry; and the field content by three scalar $SU(2)_L$ doublets $\eta = (\eta_1, \eta_2, \eta_3)$, and three right-handed (RH) neutrinos $N = (N_1, N_2, N_3)$; both as A_4 triplets [1, 3, 4]. The quantum numbers for the fields in the model are summarized in Table 1.

	L_e	L_μ	L_τ	l_e	l_μ	l_τ	N	H	η
$SU(2)_L$	**2**	**2**	**2**	**1**	**1**	**1**	**1**	**2**	**2**
$U(1)_Y$	$-\frac{1}{2}$	$-\frac{1}{2}$	$-\frac{1}{2}$	-1	-1	-1	0	$\frac{1}{2}$	$\frac{1}{2}$
A_4	**1″**	**1**	**1′**	**1″**	**1**	**1′**	**3**	**1**	**3**

Table 1: *Relevant fields and quantum numbers of the model.*

2.1 The Yukawa Sector

The lepton sector Yukawa Lagrangian of the model is

$$\mathcal{L}_{\text{Yukawa}}^{H} = y_e \overline{L}_e l_e H + y_\mu \overline{L}_\mu l_\mu H + y_\tau \overline{L}_\tau l_\tau H + h.c., \tag{1}$$

$$\mathcal{L}_{\text{Yukawa}}^{\eta} = y_1^\nu \overline{L}_e (N\tilde{\eta})_{\mathbf{1}''} + y_2^\nu \overline{L}_\mu (N\tilde{\eta})_{\mathbf{1}} + y_3^\nu \overline{L}_\tau (N\tilde{\eta})_{\mathbf{1}'} + \frac{1}{2} m_N \overline{N^c} N + h.c., \tag{2}$$

where $\tilde{\eta} = i\tau_2 \eta^\dagger$, and the subscript of the parenthesis denotes the A_4 contraction of two triplets, see [1] for details about the A_4 basis considered. Note from the last equation that due to the flavor symmetry, the three RH-neutrinos are degenerate, with mass m_N.

Since the charged leptons only couple to H, their mass matrix is diagonal and proportional to its vacuum expectation value (VEV), which we label by v_H.

$$\frac{v_H}{\sqrt{2}} Y_l^H = \frac{v_H}{\sqrt{2}} \begin{pmatrix} y_e & 0 & 0 \\ 0 & y_\mu & 0 \\ 0 & 0 & y_\tau \end{pmatrix}. \tag{3}$$

From Eq. (2) the Yukawa coupling matrices of the η fields with neutrinos are

$$Y^{\eta_1} = \begin{pmatrix} y_1^\nu & 0 & 0 \\ y_2^\nu & 0 & 0 \\ y_3^\nu & 0 & 0 \end{pmatrix}, \quad Y^{\eta_2} = \begin{pmatrix} 0 & y_1^\nu \omega^2 & 0 \\ 0 & y_2^\nu & 0 \\ 0 & y_3^\nu \omega & 0 \end{pmatrix}, \quad Y^{\eta_3} = \begin{pmatrix} 0 & 0 & y_1^\nu \omega \\ 0 & 0 & y_2^\nu \\ 0 & 0 & y_3^\nu \omega^2 \end{pmatrix}, \quad \text{with} \quad \omega = e^{i\frac{2\pi}{3}}. \tag{4}$$

We want to remark that there are only three parameters y_1^ν, y_2^ν, and y_3^ν, ruling the Yukawa interaction of neutrinos. As stated in the next section (for a detailed account, see [1]), neutrino masses are generated by a type-I seesaw and a scotogenic mechanism [5–7]. The key feature of this model, in contrast to previous works, is that it naturally predicts the dominance of the seesaw over the scotogenic mechanism [8–14].

3

2.2 Flavor Symmetry Breakdown

The A_4 symmetry is spontaneously broken at the electroweak scale by the η field. Furthermore, in the case that only η_1 acquires a VEV; there is a residual $\mathbb{Z}_2$ symmetry that stabilizes a dark matter particle candidate [3]. The VEV alignment of this model

$$\langle \eta^0 \rangle = \frac{1}{\sqrt{2}} \begin{pmatrix} v_{\eta_1} \\ 0 \\ 0 \end{pmatrix}, \qquad \langle H^0 \rangle = \frac{v_H}{\sqrt{2}}, \qquad \text{with} \quad v^2 = v_{\eta_1}^2 + v_H^2 \approx (246\,\text{GeV}), \tag{5}$$

remains invariant under one of the generators of A_4, which generates the remnant symmetry (the details are given in [1]). The denominated "dark" fields, odd under this $\mathbb{Z}_2$, are

$$\mathbb{Z}_2: \quad \eta_2 \longrightarrow -\eta_2, \quad \eta_3 \longrightarrow -\eta_3, \quad N_2 \longrightarrow -N_2, \quad N_3 \longrightarrow -N_3, \tag{6}$$

while the rest of the fields are invariant, including the SM particles, and are referred to as "active" fields.

3. Neutrino mass mechanisms

In this model, both the active and dark sectors contribute to generate the neutrino mass matrix. For the sake of clarity we will write their contributions, up to one-loop, separately:

$$(m_\nu)_{\alpha\beta} = (m_\nu^{\text{Active}})_{\alpha\beta} + (m_\nu^{\text{Dark}})_{\alpha\beta}, \qquad \text{with} \quad \alpha = e, \mu, \tau. \tag{7}$$

The fields η_1, H, N_1 and Z contribute to m_ν^{Active} through a type-I seesaw and its one-loop corrections, as it is illustrated by the Feynman diagrams in Figures 2, and 3. Furthermore their total contribution is only a rank-1 matrix, generating thus only the heaviest neutrino mass, as depicted in Figure 1 .

The dark fields fields in Eq. (6) contribute to m_ν^{Dark} through a scotogenic mechanism, as it is illustrated by the Feynman diagram in Figures 4. This mechanism yields a rank-2 matrix, generating the two lighter neutrino masses, also as depicted in Figure 1. The expressions for these contributions are given in [1].
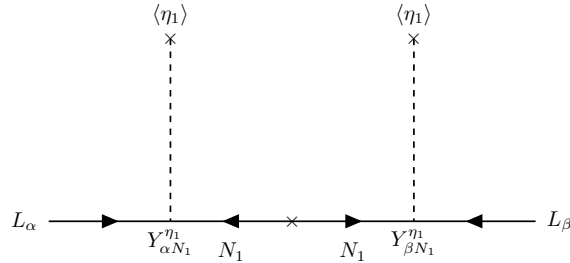

Figure 2: The active fields N_1 and η_1 take part in the seesaw mechanism. Their contribution can only generate a rank-1 mass matrix for light neutrinos. Together with its one-loop corrections in Figure 3 they generate the atmospheric mass splitting $|\Delta m_{31}^2|$ (NO).
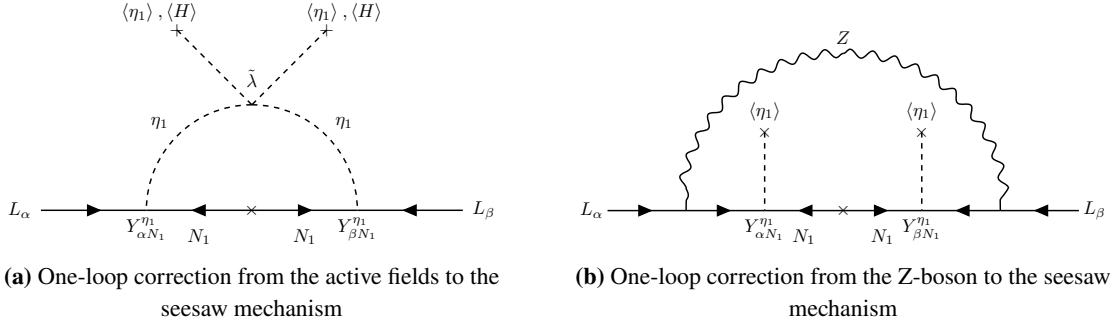
(a) One-loop correction from the active fields to the seesaw mechanism

(b) One-loop correction from the Z-boson to the seesaw mechanism

Figure 3: Corrections from the active fields η_1, N_1, and the Z-boson to the seesaw mechanism. The $\tilde{\lambda}$ represents the relevant scalar potential couplings. The scalar potential is written explicitly in [1].
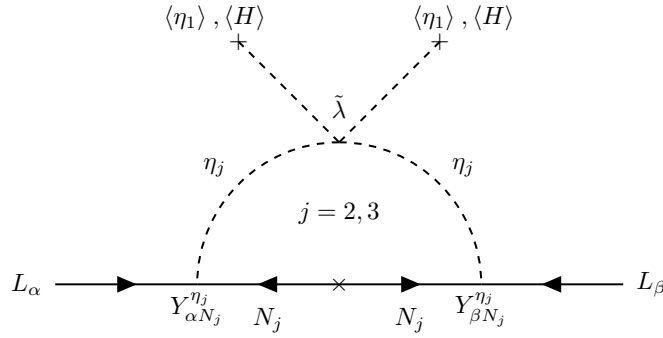

Figure 4: The dark fields N_2, N_3, η_2, and η_3 partake in the scotogenic mechanisms, the Yukawa couplings $Y^{\eta_j}_{\alpha N_j}$ for $j = 2, 3$ are written explicitly in Eq. (4). The contribution from this diagram generates a rank-2 mass matrix for light neutrinos. This contribution generates radiatively the solar mass splitting Δm^2_{21} (NO).

4. Normal Ordering of Neutrino Masses

Due to the A_4 symmetry both mass mechanism in the model share the same neutrino Yukawa couplings. As a consequence, this model predicts normal ordering (NO) for neutrino masses since the scotogenic rank-2 mass matrix m^{Dark}_ν, cannot dominate over m^{Active}_ν, which emerges at tree-level. Hence, results for inverted order (IO) are not attainable.

$$m^{\text{Active}}_\nu \quad \Longrightarrow \quad \Delta m^2_{31} \quad (\text{NO}), \qquad m^{\text{Dark}}_\nu \quad \Longrightarrow \quad \Delta m^2_{21} \quad (\text{NO}). \tag{8}$$

This comes as a result of the fact that the mass mediators for both mechanisms in this model belong to the same multiplets of the A_4 flavour symmetry.

4.1 Lepton CP phase δ^ℓ, and the lightest neutrino mass

In this model, the Yukawa couplings in Eqs. (3), and (4) can be set to be real without a loss of generality due to the A_4 symmetry

$$\{y_e,\ y_\mu,\ y_\tau,\ y^\nu_1,\ y^\nu_2,\ y^\nu_3\}, \tag{9}$$

Therefore, the discrete dark matter model has two properties concerning CP-symmetry; the first one is that lepton CP is strictly preserved at the tree-level, thus it can only emerge from the scalar

potential's CP-breaking couplings through radiative corrections, the second one is that from our analysis of the parameter space, we found that assuming CP conservation in the scalar potential is not a viable scenario, since in this case the mixing angle between the dark scalars η_2, η_3 is fixed (to $\pi/4$) and the model is unable to reproduce the observed oscillation parameters. Hence this model requires CP violation in the scalar sector to be viable. Nonetheless, the results from scanning the parameter space give values of the lepton CP-phase δ^ℓ close to lepton CP-conservation

$$\delta^\ell \sim 0,\, 2\pi, \qquad \delta^\ell \sim \pi, \tag{10}$$

as shown in Figure 5 (a). Furthermore, we find a correlation between the lightest neutrino mass $m_\nu^{\text{lightest}} = m_1^\nu$ and the solar mixing angle ($\sin^2 \theta_2 1$), and it constrains the value of m_ν^{lightest} to the range

$$2 \text{ meV} \leq m_\nu^{\text{lightest}} \leq 8 \text{ meV}, \tag{11}$$

as can be seen in Figure 5 (b).
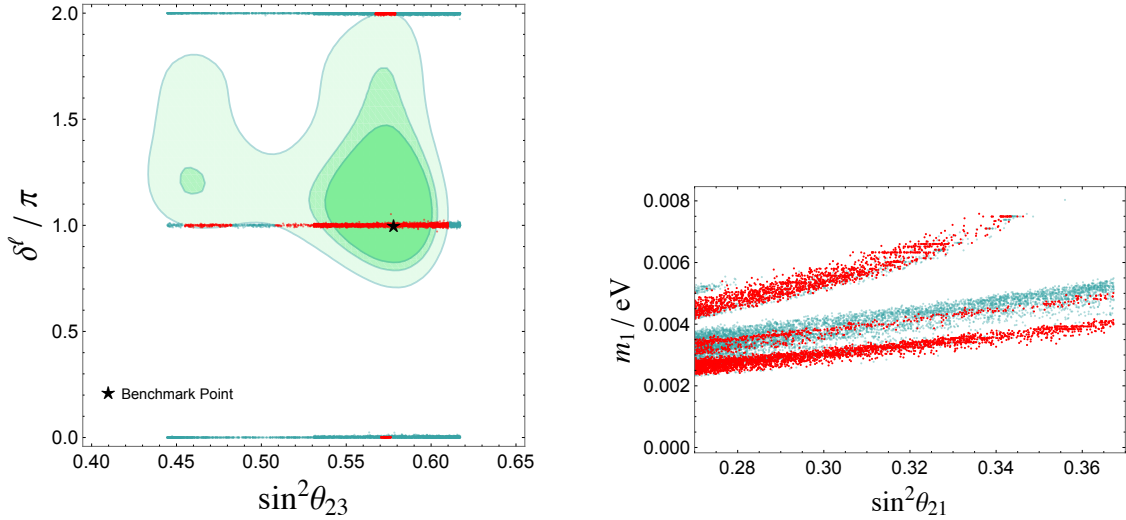
(a) The regions in different shades of green are the 90, 95, and 99% CL regions in the $\sin^2 \theta_{23}$ vs. δ^ℓ plane [2]. Table 2 displays the benchmark point data.

(b) Strong correlation between the mass of the lightest neutrino m_1^ν and $\sin^2 \theta_{21}$ in this model. This correlation constrains the m_1^ν attainable range.

Figure 5: Scatter plots of viable points from our parameter scan. The red points are inside the allowed region for δ^ℓ. The coloring of the points matches in both figures. These figures were taken directly from [1].

4.2 Dark matter and scalar spectrum

In this model, the lightest $\mathbb{Z}_2$-odd particle is a dark matter candidate. From the parameter space scan, we found that for viable lepton mixing in this model, the heavy fermion mass m_N is much larger than that of the neutral dark scalars. Hence this model has a scalar as WIMP dark matter candidate with a mass of the order of the electroweak scale. Furthermore, the scalar spectrum is very rich in this model. Since there are four scalar $SU(2)$ doublets in the model, to illustrate it, we summarize the results for the scalar field spectrum in Table 3. More details and results about the analysis of the scalar sector are in [1].

Observable	Data		Best fit
	Central value	1σ range	
$\sin^2\theta_{12}/10^{-1}$	3.18	$3.02 \to 3.34$	3.03
$\sin^2\theta_{13}/10^{-2}$ (NO)	2.200	$2.138 \to 2.269$	2.201
$\sin^2\theta_{23}/10^{-1}$ (NO)	5.74	$5.60 \to 5.88$	5.78
δ^ℓ/π (NO)	1.08	$0.96 \to 1.21$	1.0
$\Delta m_{21}^2/(10^{-5}\,\mathrm{eV}^2)$	7.50	$7.30 \to 7.72$	7.53
$\Delta m_{31}^2/(10^{-3}\,\mathrm{eV}^2)$ (NO)	2.55	$2.52 \to 2.57$	2.55
$m_{\mathrm{lightest}}^\nu$ /meV (NO)			5.57
m_2^ν /meV			10.37
m_3^ν /meV			50.87
ϕ_{12}/π			1.5
ϕ_{13}/π			1.5
ϕ_{23}/π			1.0
$\langle m_{\beta\beta}\rangle/\mathrm{eV}$			3.15×10^{-4}
m_e /MeV	0.486	$0.486 \to 0.486$	0.486
m_μ /GeV	0.102	$0.102 \to 0.102$	0.102
m_τ /GeV	1.746	$1.743 \to 1.747$	1.746
v_{η_1} /GeV			84.6
v_H /GeV			231.0
v /GeV	246	$246 \to 246$	246
M_H /GeV (Higgs)	125.25	$125.08 \to 125.42$	125.25

Table 2: Model parameters and corresponding observables for this benchmark point.

Scalar field	Data		Model best fit
	Central value	1σ range	
M_H /GeV (Higgs boson)	125.25	$125.08 \to 125.42$	125.25
M_{DM} /GeV (lightest dark scalar)			60.00
M_{H_0} /GeV (Heavy Higgs)			294.86
M_{A_0} /GeV (Heavy Pseudoscalar)			402.41
$M_{H_0}^+$ /GeV (Charged Active)			313.81
$M_{\chi_1^+}$ /GeV (Charged Dark)			482.3
$M_{\chi_2^+}$ /GeV (Charged Dark)			341.11
$M_{\chi_1}^0$ /GeV (Neutral Dark)			324.04
$M_{\chi_2}^0$ /GeV (Neutral Dark)			322.44
$M_{\chi_3}^0$ /GeV (Neutral Dark)			82.4

Table 3: Benchmark point values for the masses of the scalar fields in the model.

5. Conclusions

In this work [1], we have studied the discrete dark matter model (DDM), which is based on a A_4 flavor symmetry in the lepton sector, where the interplay between the seesaw and scotogenic mechanisms arises directly from a remnant symmetry of the spontaneous A_4 breaking. This residual symmetry stabilizes a scalar dark matter candidate.

The model has the unique property among the scoto-seesaw models, the Yukawa couplings ruling both mechanisms are the same. Therefore tree-level seesaw dominates over the one-loop scotogenic mechanism due to the A_4 flavor symmetry. Consequently the model predicts normal ordering (NO) for neutrino masses, favored by neutrino oscillation experiments. The only source of leptonic CP-violation originates in the scalar potential. Furthermore, the latter is necessary to obtain lepton mixing parameters consistent with the current experimental values. The values obtained for

the Dirac CP-phase lie close to the CP-preserving values, as displayed in Figure 5. There is a strong correlation between the mass of the lightest neutrino mass (NO) and the solar mixing angle, which constrains m_1^ν to be between $2\,\text{meV} \lesssim m_{\text{lightest}}^\nu \lesssim 8\,\text{meV}$. The model contains a rich scalar sector with charged and neutral states, accessible to collider experiments. Previous works on the DDM model explore this sector [3, 4].

Acknowledgments

References

[1] C. Bonilla, J. Herms, O. Medina and E. Peinado, *Discrete dark matter mechanism as the source of neutrino mass scales*, arXiv:2301.10811 [hep-ph].

[2] P. F. de Salas et al., *2020 global reassessment of the neutrino oscillation picture*, JHEP **02** (2021) 071, arXiv:2006.11237 [hep-ph].

[3] M. Hirsch, S. Morisi, E. Peinado and J. W. F. Valle, *Discrete dark matter*, Phys. Rev. D **82** (2010) 116003, arXiv:1007.0871 [hep-ph].

[4] M. S. Boucenna et al., *Phenomenology of Dark Matter from A_4 Flavor Symmetry*, JHEP **05** (2011) 037, arXiv:1101.2874 [hep-ph].

[5] J. Schechter and J. W. F. Valle, *Neutrino Masses in SU(2) x U(1) Theories*, Phys. Rev. D **22** (1980) 2227.

[6] E. Ma, *Verifiable radiative seesaw mechanism of neutrino mass and dark matter*, Phys. Rev. D **73** (2006) 077301, arXiv:hep-ph/0601225.

[7] P. Escribano, M. Reig and A. Vicente, *Generalizing the Scotogenic model*, JHEP **07** (2020) 097, arXiv:2004.05172 [hep-ph].

[8] N. Rojas, R. Srivastava and J. W. F. Valle, *Simplest Scoto-Seesaw Mechanism*, Phys. Lett. B **789** (2019) 132–136, arXiv:1807.11447 [hep-ph].

[9] A. Aranda, C. Bonilla and E. Peinado, *Dynamical generation of neutrino mass scales*, Phys. Lett. B **792** (2019) 40–42, arXiv:1808.07727 [hep-ph].

[10] A. Ibarra and C. Simonetto, *Understanding neutrino properties from decoupling right-handed neutrinos and extra Higgs doublets*, JHEP **11** (2011) 022, arXiv:1107.2386 [hep-ph].

[11] D. M. Barreiros, F. R. Joaquim, R. Srivastava and J. W. F. Valle, *Minimal scoto-seesaw mechanism with spontaneous CP violation*, JHEP **04** (2021) 249, arXiv:2012.05189 [hep-ph].

[12] D. M. Barreiros, H. B. Camara and F. R. Joaquim, *Flavour and dark matter in a scoto/type-II seesaw model*, JHEP **08** (2022) 030, arXiv:2204.13605 [hep-ph].

[13] S. Mandal, R. Srivastava and J. W. F. Valle, *The simplest scoto-seesaw model: WIMP dark matter phenomenology and Higgs vacuum stability*, Phys. Lett. B **819** (2021) 136458, arXiv:2104.13401 [hep-ph].

[14] J. Ganguly, J. Gluza and B. Karmakar, *Common origin of θ_{13} and dark matter within the flavor symmetric scoto-seesaw framework*, JHEP **11** (2022) 074, arXiv:2209.08610 [hep-ph].